For submission to the AEGIS ApJL Special Issue

A Strong-Lens Survey in AEGIS: the influence of large scale structure

Leonidas A. Moustakas[1]

Phil Marshall[2]

Jeffrey A. Newman[3,11]

Alison L. Coil[4,12]

Michael C. Cooper[5]

Marc Davis[5]

Christopher D. Fassnacht[6]

Puragra Guhathakurta[8]

Andrew Hopkins[9]

Anton Koekemoer[10]

Nicholas P. Konidaris[8]

Jennifer M. Lotz[11,13]

Christopher N. A. Willmer[4]

ABSTRACT

We report on the results of a visual search for galaxy-scale strong gravitational lenses over 650 arcmin^2 of *HST*/ACS (F606W and F814W) imaging in the DEEP2-Extended Groth Strip (EGS). In addition to a previously-known Einstein Cross also found by our search (the "Cross," HST J141735+52264, $z_{\rm lens} = 0.8106$, $z_{\rm source} = 3.40$), we identify two new strong galaxy-galaxy lenses with multiple extended arcs. The first, HST J141820+52361 (the "Dewdrop"; $z_{\rm lens} = 0.5798$), lenses two distinct extended sources into two pairs of arcs ($z_{\rm source} = 0.9818$), while the second, HST J141833+52435 (the "Anchor"; $z_{\rm lens} = 0.4625$), produces a single pair of arcs ($z_{\rm lens}$ not yet known). Four less convincing arc/counter-arc and two-image lens candidates are also found and presented for completeness. Lenses are found in a both underdense and overdense local environments, as characterized by a robust measure, $1+\delta_3$, a normalized density that uses the distance to the third nearest neighbor. All three definite lenses are fit reasonably well by simple singular isothermal ellipsoid models including external shear, giving χ^2_ν values close to unity. These shears are much greater than those implied by a simple consideration of the three-dimensional convergence and shear from galaxies along the line of sight, where each galaxy is approximated by a singular isothermal sphere halo truncated at $200\,h^{-1}$ kpc. This shows how a realistic treat-

[1]JPL/Caltech, 4800 Oak Grove Dr, MS 169-327, Pasadena, CA 91109 leonidas@jpl.nasa.gov

[2]KIPAC, P.O. Box 20450, MS29, Stanford, CA 94309; Physics Dept, Broida Hall, MC9530, UC Santa Barbara, Santa Barbara, CA 93106

[3]INPA, LBNL, Berkeley, CA 94720

[4]S.O., University of Arizona, Tucson, AZ 85721

[5]Department of Astronomy, U.C. Berkeley, Berkeley, CA 94720

[6]Department of Physics, U.C. Davis, Davis, CA 95616

[7]Department of Physics, U.C. Berkeley, Berkeley, CA 94720

[8]U.C.O./Lick Observatory, UCSC, Santa Cruz, CA 95064

[9]School of Physics, University of Sydney NSW, Australia

[10]Space Telescope Science Institute, Baltimore, MD 21218

[11]NOAO, 950 North Cherry Street, Tucson, AZ 85719

[12]*Hubble* Fellow

[13]Goldberg Fellow

ment of galaxies and the large scale structure they are embedded in is necessary, and that simply characterizing the very-local environment may be insufficient.

Subject headings: gravitational lensing – galaxies: high-redshift – large-scale structure of universe – galaxies: individual (HST J141735+52264) – galaxies: individual (HST J141820+52361) – galaxies: individual (HST J141833+52435)

1. Introduction

Galaxy-scale gravitational lenses have many astrophysical and cosmological applications. These rely on the ability to construct robust and accurate gravitational lens models. However, the contribution of the large-scale structure along the line of sight (LOS) between the observer and the source is often unknown, though it may be significant. In particular, though lens models may detect the influence of the distorting effects of environmental shear (γ) in a preferred direction, models of even the most richly-constrained Einstein Rings with *Hubble Space Telescope* images (e.g. Dye & Warren 2005; Wayth et al. 2005; Koopmans et al. 2006) are still subject to the mass-sheet degeneracy due to extra field convergence (κ), which can lead to incorrect lens masses (e.g. Kochanek 2004). Indeed, lens galaxies are often massive early-type galaxies, which are generally found in groups or clusters. The most famous example is the two-image lensed QSO Q0957+561 (Walsh et al. 1979; Young et al. 1980). The determination of H_0 from this system depends crucially on correctly modeling the galaxy cluster surrounding the primary lensing galaxy (e.g. Keeton et al. 2000). Several other lens-galaxy groups and environments have been studied in detail (Kundic et al. 1997a,b; Tonry 1998; Tonry & Kochanek 1999; Fassnacht & Lubin 2002; Morgan et al. 2005; Williams et al. 2005; Momcheva et al. 2006; Fassnacht et al. 2006a; Auger et al. 2006), with sometimes inconclusive results. In analyses such as in Keeton & Zabludoff (2004), through mock lens realizations, it is shown how local environment may affect key applications of lenses. They argue that H_0 and Ω_Λ may be overestimated, the expected ratio of four-image to two-image lenses may be underestimated, and predictions for millilensing by dark matter substructure may be off by significant amounts. Other theoretical work (Bar-Kana 1996; Metcalf 2005; Wambsganss et al. 2005; Das & Ostriker 2006) suggests that *all* matter along a line of sight can be important.

In the emergent era of large-solid angle, densely-sampled spectroscopic surveys that may include strong lenses, both environmental and large-scale structure effects can be explored quantitatively. The DEIMOS spectroscopy of the Extended Groth Strip (EGS) is particularly well-suited to this task, and is employed here to both discover new strong galaxy-lenses, and to begin addressing the quantitative effect of environment in their behavior.

The DEEP2-EGS field is a 120×30 arcmin strip, the focus of the "All-wavelength EGS International Survey" (AEGIS), includes deep CFHT BRI imaging (Coil et al. 2004a) and Keck/DEIMOS spectroscopy of nearly 14 000 galaxies to date. The spectroscopy is $\sim 75\%$ complete to $R_{\rm AB} < 24.1$. For the analysis here, we only employ the most certain redshift assignments (Coil et al. 2004b). Deep *HST*/ACS imaging of nearly 650 arcmin^2 over 63 stitched tiles reach $V_{606} = 28.75$ and $I_{814} = 28.10$ (AB, 5σ point source; Davis et al, this issue). These data lend themselves to two different techniques for searching for heretofore-unknown gravitational lenses: spectroscopically and visually. The spectroscopic redshifts are supplemented as necessary with photometric redshifts measured from deep KPNO $UBVRI$ imaging (A. Hopkins et al., in prep).

The spectroscopic approach of searching for "anomalous" emission lines in early-type spectra has some history (e.g. Warren et al. 1996), and has recently proved to be spectacularly successful when applied to SDSS spectroscopy (Bolton et al. 2004; Willis et al. 2005) with *HST*/ACS followup (Bolton et al. 2005, 2006; Treu et al. 2006). Explicitly spectroscopic searches for lenses in the DEEP2 data will be explored elsewhere.

In the imaging domain, one may hope to search for lens candidates by some automated algorithm, or by visual inspection (e.g. Ratnatunga et al. 1995; Zepf et al. 1997; Fassnacht et al. 2004). The more quantitative and objective automated approach may eventually be preferred (especially for datasets larger than the one considered here), but would, however, require a training set. The EGS ACS data described here is used for just this purpose in a separate work (Marshall et al. in prep) as a precursor to searching the entire *HST* imaging dataset.[1] Towards that goal we have undertaken a search for lenses by purely visual inspection.

The lens-search methodology is described in § 2. The newly discovered lenses and the modeling results are given in § 3, while measurements of the local and LOS environments of the lenses are given in § 4. Discussion and conclusions are the subject of § 5. A concordance flat cosmology with $\Omega_\Lambda = 1 - \Omega_{\rm m} = 0.7$ and $H_0 = 100\,h\,{\rm km\,s^{-1}\,Mpc^{-1}}$ with $h = 0.7$ is used throughout. Unless otherwise stated, all magnitudes are in the AB system.

2. Lens-search methodology

The search for gravitational lens candidates was conducted by-eye. Three-color images of all of the ACS tiles were built following the Lupton et al. (2004) algorithm, using the

[1] `http://www.slac.stanford.edu/~pjm/HAGGLeS`

photometric zeropoints to provide the relative scale factors, and using the mean of the F606W and F814W images for the green channel. The full ACS dataset was inspected repeatedly in the color images at full resolution, with plausible candidates classified with grades of "A" or "B" and marked for further inspection. Object coordinates were then matched against the DEEP2 spectroscopic catalog, which includes a "serendipitous feature" flag, for possible anomalous, higher-redshift emission lines. Emission from a source behind the Dewdrop lens (described below) was found in this way.

3. Lenses & Models

In addition to a previously known Einstein Cross, we find two new unambiguous strong galaxy-galaxy lenses (Fig. 1), all three of which are discussed below. Four additional plausible lens candidates are also reported (Fig. 2).

3.1. Lens modeling and source reconstruction

The lensed sources in the EGS all appear to be blue and extended, and are likely star forming galaxies at high redshift ($z \sim 1$). We therefore take the image pixels as our data (rather than simply image-centroid positions), and predict the image using a simple ray tracing forward from the source plane, followed by a PSF convolution. We first subtract the lens galaxy light using a tilted 2D Moffat profile,[2] and mask the very center of the lens galaxy where some residual flux remains. It is important that the unmasked region contain not only the lensed images but also the clean pixels that do *not* have lensed features. These clean pixels contain at least as much information as the ones with lensed flux, vetoing models that predict images where there are none. For the projected mass profile of the lens we adopt a singular isothermal ellipsoid (SIE; Kormann et al. 1994) model, plus an external shear component. Using a Markov chain Monte Carlo procedure presented in detail elsewhere (Marshall et al. in prep), the position, ellipticity, orientation and mass of the lens, external shear amplitude and the direction, position, ellipticity, orientation and Sersic profile parameters of the source are all fit to the data. Since we are interested in accurate estimation of the lens environment, we apply a prior on the orientation of the lens ellipticity to reflect the expected correlation with the lens light (e.g. Koopmans et al. 2006).

[2]The Moffat function is a modified Lorentzian with variable power law index. The fit is done with the `MPFIT` IDL suite of C. Markwardt.

3.2. HST J141735+52264 (A1 – Cross)

This lens was originally discovered by Ratnatunga et al. (1995) by visual inspection of the *HST*/WFPC2 Medium Deep Survey (MDS) data. The lens redshift is $z_{\rm lens} = 0.8106$ (Table 1), and the source is at $z_{\rm source} = 3.4$ (Crampton et al. 1996). The large Einstein radius $\theta_{\rm E} = 1.447$ arcsec and the four-image configuration require a large enclosed mass and a significant amount of external shear, $\gamma_{\rm mod} = 0.080$, a result consistent with Treu & Koopmans (2004). The best-fit model shows very small residuals at the two outer images, a feature corrected for by Treu & Koopmans (2004) with a potential gradient that is presumably associated with a nearby structure. The mass and external shear are not affected by this correction.

3.3. HST J141820+52361 (A2 – Dewdrop)

The Dewdrop lens at $z_{\rm lens} = 0.5798$ lenses two distinct sources into two pairs of arcs. The Keck/DEIMOS spectrum of the system reveals anomalous [O II] nebular emission at $z_{\rm source} = 0.9818$ (Fig. 3). The sources in the Dewdrop system are part of a remarkable irregular and loose association of star formation knots and diffuse emitting material that extends over more than 10 arcsec, or more than 80 kpc comoving in size.

3.4. HST J141833+52435 (A3 – Anchor)

The Anchor system exhibits a pair of arcs created by a lens at a redshift of $z_{\rm lens} = 0.4625$. The best-fitting lens model requires a significant external shear contribution (see Table 1), as might be expected from the position and shape of the counter-image to the main arc.

3.5. Additional lens candidates

In Fig. 2 and Table 1 we identify four additional visually-identified lens candidates. Only two of the four presently have redshifts measured, and require further spectroscopic followup. These are presented for completeness, and do not affect the scope or results of this paper.

4. The Environments of the Lenses

We explore the environments of the lenses in two different ways. The first makes use of a relatively unbiased measure of the very local environment of any one galaxy, dubbed $1+\delta_3$ and explored in detail in Cooper et al. (2005a,b). This parameter is derived from the distance to the third-nearest neighbor among the galaxies within $1000\,\mathrm{km\,s^{-1}}$ along the line of sight, and scales as the inverse of the cube of this distance. More concentrated environments have larger values of $1+\delta_3$, with typical uncertainties of ~ 0.5 dex. We only compute this measure for galaxies with spectroscopic redshifts.

As a second probe of lens environment we model the contribution to the lensing potential due to individual neighboring galaxies using simple analytic mass distributions. We calculate the convergence $\kappa_{\rm los}$ and shear $\gamma_{\rm los}$ line-of-sight contribution by all galaxies within a projected separation of $200\,h^{-1}$ kpc from the lens galaxies, out to the redshift of the source. We treat each galaxy as an isolated halo, undoubtedly neglecting the effect of group halos and other structures. Assuming that we can approximate each galaxy i as a singular isothermal sphere (SIS), we have $\kappa_i = b_i/2r_i$, where r is the projected distance from the lens and b is the "lens strength" for a background source at angular diameter distances of $D_{\rm s}$ from the observer and $D_{\rm ls}$ from the lens, $b = 4\pi\,(\sigma_{\rm dm}/c)^2\,D_{\rm ls}/D_{\rm s}$. The central dark matter velocity dispersion $\sigma_{\rm dm}$ of each galaxy is assumed to be the same as the central stellar velocity dispersion, which is derived from the estimated rest-frame B-band (Vega) magnitude of each galaxy using the Faber-Jackson relationship as given in Mitchell et al. (2005) (see also Jönsson et al. 2006). (We neglect the dispersion in this relation). The total shear contribution is the "headless-vector" sum of the shears, $\bar{\gamma}_{\rm los} = \Sigma\bar{\gamma}_i$, while the total convergence is a scalar sum: $\kappa_{\rm los} = \Sigma\kappa_i$. It is worth noting that if at large radii the profiles are steeper than SIS (such as NFW), the convergence contribution will be smaller overall than the shear. These measurements are given in Table 1 and discussed in the last section.

5. Discussion & Conclusions

The numbers of definite lenses reported on here is consistent with other surveys. For example, Bolton et al. (2006) find that $\sim$0.1% of luminous red galaxies are very likely to be strong galaxy-galaxy lenses, although special lines of sight can have much higher lensing rates (e.g. Fassnacht et al. 2006b). The rate above then suggests that there should be $\sim$4 strong lenses in this survey, which is a good match to the three lenses found in our survey.

The main conclusions of this work can be drawn by an examination of Fig. 4. The lower panel shows the local-environmental $1+\delta_3$ and the shear values for the lenses. The Cross is in

an overdense local environment, consistent with this lens being associated with the $z \approx 0.8$ sheet described in Koo et al. (1996) and Im et al. (2002). The shear of $\sim$10% required by the model (see also Treu & Koopmans 2004), then, seems acceptable. The other two lenses are in statistically *under*-dense environments. The upper panel of Fig. 4 shows two shears for each lens, one derived from the full lens modeling, and another estimated as in Sec. 4. In all cases, the former shears are much greater than the latter. The natural conclusion is that the cartoon assumption of large isolated SIS galaxies is grossly insufficient, so there must be much more mass unaccounted for. To explore this further, we ran lens models with external shear and orientation *restricted to the "predicted" values*. All three new models require lenses with much higher ellipticity than the light suggests, though in the Dewdrop and the Anchor the formal χ^2_ν remains plausible given the constraints, $\chi^2_\nu = 1.02$ and 1.04 (or underfit by $\sim$1- and $\sim$2-σ), respectively. The new Cross fit, however, is strongly ruled out with $\chi^2_\nu = 2.00$ (or by $\sim$75-σ). This suggests that at least in this case, the inferred LOS influence by SIS dark matter halos is clearly insufficient, and that the large-scale structure "sheet" must have an important additional effect.

Our conclusions may be summarized as follows: **1.** *We have discovered two new strong galaxy-galaxy lenses by visual inspection, with reasonable lens models and source reconstructions. This shows the potential for discovering many more strong lenses in existing* HST *data.* **2.** *While these lenses are found in a broad range of spectroscopically-determined local-density environments, the lens modeling requires comparable levels of external shear for each lens. This suggests that a determination of immediately-local environment is insufficient for characterizing the influence of external galaxies on lenses. Since external shear and convergence are related, this in turn has implications for how reliable estimates of the average external convergence in other lenses can be.* **3.** *In all lenses but especially in the case of the Cross, a simple model of the effect of LOS "SIS" galaxies produces insufficient levels of shear, as required for good lens model fits. More sophisticated consideration of galaxies' halos and large scale structure is necessary.*

We thank Maruša Bradač for discussions. The work of LAM was carried out at Jet Propulsion Laboratory, California Institute of Technology, under a contract with NASA. JAN and ALC are supported by NASA through the *Hubble* Fellowship grants HF-011065.01-A and HF-01182.01-A, respectively. The work of PJM was supported in part by the U.S. Department of Energy under contract number DE-AC02-76SF00515. LAM thanks Russell Mirabelli for expert assistance with a script facilitating the inspection of the ACS data, and UC Berkeley and UC Santa Cruz for their frequent hospitality during the course of this work.

REFERENCES

Auger, M. W., Fassnacht, C. D., Abrahamse, A. L., Lubin, L. M., & Squires, G. K. 2006, astro-ph/0603448

Bar-Kana, R. 1996, ApJ, 468, 17

Bolton, A. S., Burles, S., Koopmans, L. V. E., Treu, T., & Moustakas, L. A. 2005, ApJL, 624, 21

—. 2006, ApJ, 0, 0

Bolton, A. S., Burles, S., Schlegel, D. J., Eisenstein, D. J., & Brinkmann, J. 2004, AJ, 127, 1860

Coil, A. L., Newman, J. A., Kaiser, N., Davis, M., Ma, C.-P., Kocevski, D. D., & Koo, D. C. 2004a, ApJ, 617, 765

Coil, A. L., et al. 2004b, ApJ, 609, 525

Cooper, M. C., Newman, J. A., Madgwick, D. S., Gerke, B. F., Yan, R., & Davis, M. 2005a, ApJ, 634, 833

Cooper, M. C., et al. 2005b, ArXiv Astrophysics e-prints

Crampton, D., Le Fevre, O., Hammer, F., & Lilly, S. J. 1996, A&A, 307, L53

Das, S., & Ostriker, J. P. 2006, ApJ, 645, 1

Dye, S., & Warren, S. J. 2005, ApJ, 623, 31

Fassnacht, C. D., Gal, R. R., Lubin, L. M., McKean, J. P., Squires, G. K., & Readhead, A. C. S. 2006a, ApJ, 642, 30

Fassnacht, C. D., & Lubin, L. M. 2002, AJ, 123, 627

Fassnacht, C. D., Moustakas, L. A., Casertano, S., Ferguson, H. C., Lucas, R. A., & Park, Y. 2004, ApJL, 600, L155

Fassnacht, C. D., et al. 2006b, ArXiv Astrophysics e-prints

Im, M., et al. 2002, ApJ, 571, 136

Jönsson, J., Dahlén, T., Goobar, A., Gunnarsson, C., Mörtsell, E., & Lee, K. 2006, ApJ, 639, 991

Keeton, C. R., Falco, E. E., Impey, C. D., Kochanek, C. S., Lehár, J., McLeod, B. A., Rix, H.-W., Muñoz, J. A., & Peng, C. Y. 2000, ApJ, 542, 74

Keeton, C. R., & Zabludoff, A. I. 2004, ApJ, 612, 660

Kochanek, C. S. 2004, astro-ph/0407232

Koo, D. C., et al. 1996, ApJ, 469, 535

Koopmans, L. V. E., Treu, T., Bolton, A. S., Burles, S., & Moustakas, L. A. 2006, ApJ, 0, 0

Kormann, R., Schneider, P., & Bartelmann, M. 1994, A&A, 284, 285

Kundic, T., Cohen, J. G., Blandford, R. D., & Lubin, L. M. 1997a, AJ, 114, 507

Kundic, T., Hogg, D. W., Blandford, R. D., Cohen, J. G., Lubin, L. M., & Larkin, J. E. 1997b, AJ, 114, 2276

Lupton, R., Blanton, M. R., Fekete, G., Hogg, D. W., O'Mullane, W., Szalay, A., & Wherry, N. 2004, PASP, 116, 133

Metcalf, R. B. 2005, ApJ, 629, 673

Mitchell, J. L., Keeton, C. R., Frieman, J. A., & Sheth, R. K. 2005, ApJ, 622, 81

Momcheva, I., Williams, K., Keeton, C., & Zabludoff, A. 2006, ApJ, 641, 169

Morgan, N. D., Kochanek, C. S., Pevunova, O., & Schechter, P. L. 2005, AJ, 129, 2531

Ratnatunga, K. U., Ostrander, E. J., Griffiths, R. E., & Im, M. 1995, ApJL, 453, 5

Tonry, J. L. 1998, AJ, 115, 1

Tonry, J. L., & Kochanek, C. S. 1999, AJ, 117, 2034

Treu, T., Koopmans, L. V., Bolton, A. S., Burles, S., & Moustakas, L. A. 2006, ApJ, 640, 662

Treu, T., & Koopmans, L. V. E. 2004, ApJ, 611, 739

Walsh, D., Carswell, R. F., & Weymann, R. J. 1979, Nature, 279, 381

Wambsganss, J., Bode, P., & Ostriker, J. P. 2005, ApJL, 635, L1

Warren, S. J., Hewett, P. C., Lewis, G. F., Moller, P., Iovino, A., & Shaver, P. A. 1996, MNRAS, 278, 139

Wayth, R. B., Warren, S. J., Lewis, G. F., & Hewett, P. C. 2005, MNRAS, 360, 1333

Williams, K. A., Momcheva, I., Keeton, C. R., Zabludoff, A. I., & Lehar, J. 2005, astro-ph/0511593

Willis, J. P., Hewett, P. C., & Warren, S. J. 2005, MNRAS, 363, 1369

Young, P., Gunn, J. E., Oke, J. B., Westphal, J. A., & Kristian, J. 1980, ApJ, 241, 507

Zepf, S. E., Moustakas, L. A., & Davis, M. 1997, ApJL, 474, L1

Table 1: EGS lenses: data, environment, & models

		Data						Environment					Models				
ID	Alias	RA (J2000)	Dec (J2000)	$z_{\rm lens}$	R (AB)	$M_{\rm B}^{c}$ (AB)	$z_{\rm source}$	$\log(1+\delta_3)$	$\rm N_{los}$	$\kappa_{\rm los}$	$\gamma_{\rm los}$	$\theta_{\gamma_{\rm los}}$ (°E)	$\theta_{\rm E}$ ($''$)	$\sigma_{\rm SIS}$ km s^{-1}	$\gamma_{\rm mod}$	$\theta_{\gamma_{\rm mod}}$ (°E)	χ^2_ν
A1	Cross	14:17:35.72	52:26:46.3	0.8106	21.38	−21.25	3.40	+1.453	36	0.17	0.02	78	1.45	292.8	0.080	115.3	1.081
A2	Dewdrop	14:18:20.77	52:36:11.3	0.5798	20.55	−20.35	0.9818	−1.260	46	0.10	0.02	140	0.67	260.6	0.071	101.4	1.005
A3	Anchor	14:18:33.11	52:43:52.6	0.4625	20.45	−19.47	...	−0.960	52	0.09	0.02	146	0.83	248.9	0.153	140.8	0.933
B1	Flourish	14:18:07.32	52:30:29.8	0.847[a]	22.58	(−17.8)	...	...	...	...	...	...	...	...	...	...	...
B2	Quotes	14:20:52.01	53:06:57.2	0.601[b]	23.82	(−16.8)	...	...	...	...	...	...	...	...	...	...	...
B3	Dots	14:17:59.01	52:35:14.8	0.6863	21.50	−20.24	...	+0.109	...	...	...	...	...	...	...	...	...
B4	Colon	14:20:53.89	53:06:07.0	0.3545	20.61	−18.47	...	+0.880	...	...	...	...	...	...	...	...	...

a: $\sigma_z = 0.067$ & *b*: $\sigma_z = 0.24$ (A. Hopkins et al., in prep); *c*: parenthetical quantities are based on photometric redshifts.

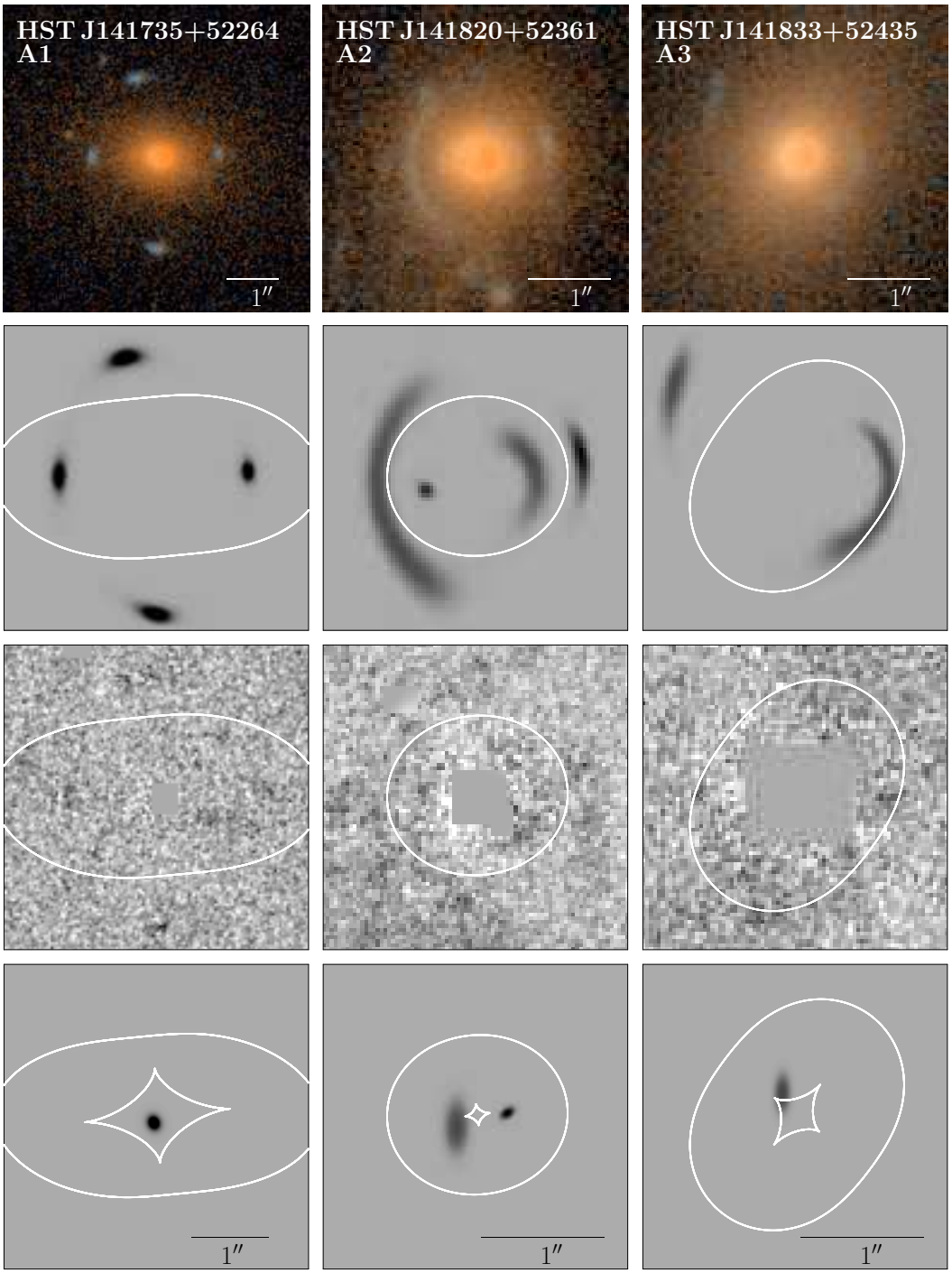

Fig. 1.— The three most plausible lenses from this survey, from left to right the Cross, the Dewdrop, and the Anchor (see text). From top to bottom, we show the discovery image, the lensed image model, the residuals by subtraction with the (lens-galaxy-removed) imaging data, and the reconstructed source. All panels, including the source-plane one, are approximately 4 arcsec on a side, with the exact dimensions shown by the scale bars. The image-plane critical curves and the source-plane caustics are shown in the third and fourth rows, respectively.

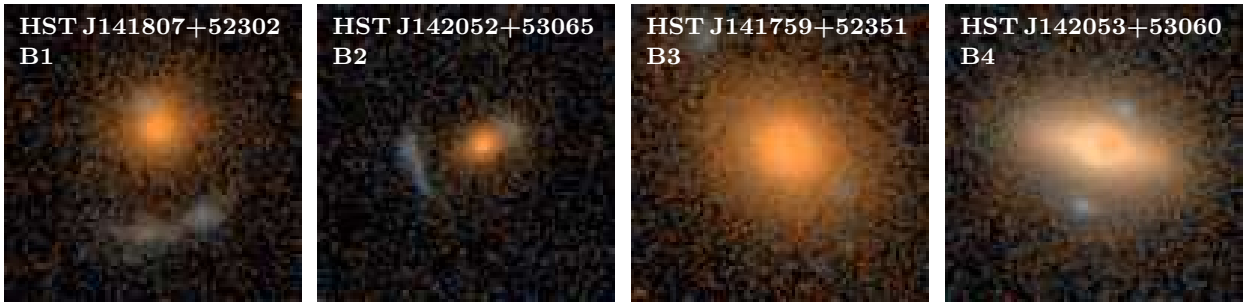

Fig. 2.— Additional lens candidates based on visual inspection, but not yet bolstered by spectroscopy. The left two are candidate arc/counter-arc lenses, whereas the right two are candidate two-image lenses. Images are 3 arcsec square.

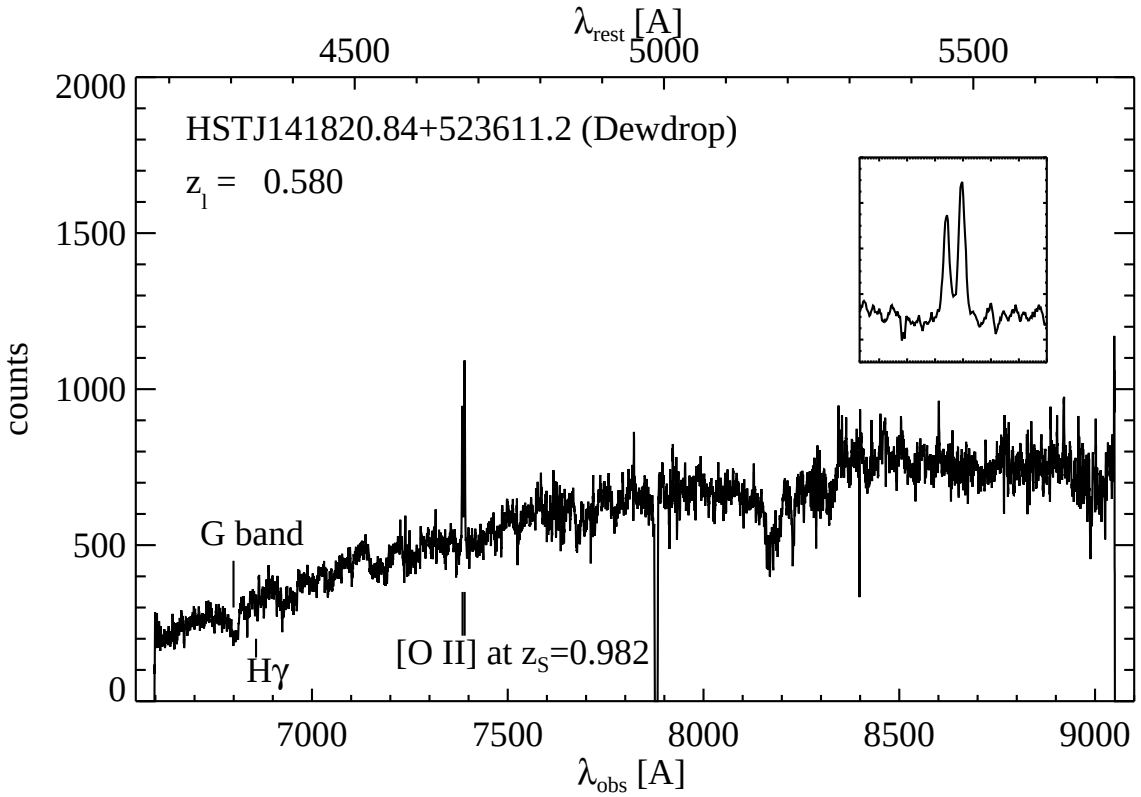

Fig. 3.— The DEIMOS spectrum of the Dewdrop lens clearly shows an "anomalous" doublet emission line (insert), which is readily identified as [O II] at $z_{\rm source} = 0.9818$.

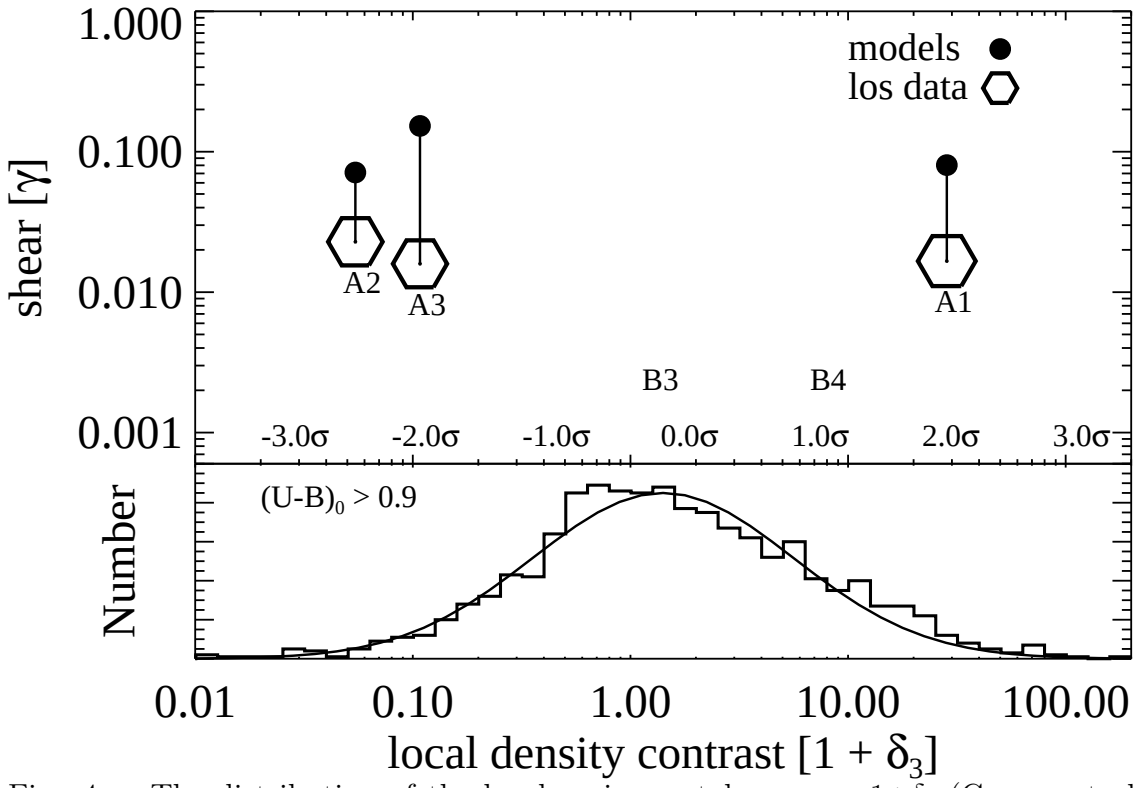

Fig. 4.— The distribution of the local-enviromental measure $1+\delta_3$ (Cooper et al. 2005a), for "red sequence" galaxies with rest-frame colors $(U-B)_0 > 0.9$ (valid for all lenses here), including $N\,\sigma$ deviations from the mean. **Upper panel:** The shear for each lens, inferred through the lens models (filled-circles), and through the simple SIS-based line-of-sight influence (open hexagons). The $1+\delta_3$ values of the lens-candidates B3 and B4 are shown as well.